International Journal of Research in Advanced Engineering and Technology
ISSN: 2455-0876
Impact Factor: RJIF 5.44
www.newengineeringjournal.in
Volume 4; Issue 3; September 2018; Page No. 13-17

Optimization of tensile-shear load of friction stir spot welded AA1050-O/AA6061-T4 aluminum sheets using design of experiment approach

Bader D Al-Mutairi[1], SS Mohamed[2], SA Abdallah[3]
[1-3] Mechanical Engineering Department, Faculty of Engineering at Shoubra, Benha University, Cairo, Egypt

Abstract
In the present investigation, 2 mm sheets of AA1050-O and AA6061-T4 were joined using friction stir spot welding (FSSW). The influences of tool rotational speed, dwell time and plugging depth on the tensile-shear force of FSSW lap joints were determined. The FSSW were performed using a tool with a taper pin profile and concave shoulder surface. The analysis of variance (ANOVA) approach was used as a statistical design of experiment technique to set the optimal FSSW parameters that maximize the tensile-shear load of AA1050-O/AA6061-T4 dissimilar lap joints and also to determine the contribution of each FSSW parameter. The results revealed that tool rotational speed has the most significant statistical and physical effect on the tensile-shear load of AA1050-O/AA6061-T4 dissimilar lap welded joints. The optimum FSSW process parameter that maximize the tensile-shear load are at tool rotational speed, dwell time and plunging depth of 710 rpm, 7 sec. and 3.05 mm, respectively.

Keywords: friction stir spot welding, aluminum alloys, tensile-shear load, ANOVA

1. Introduction

The friction stir spot welding (FSSW) was developed, in 2001, to replace the resistance spot welding (RSW) for aluminum alloys. The FSSW has several advantages over RSW [1, 3]. The FSSW have much lower operating costs, higher energy efficiency (over 90% power saving) and less equipment costs (over 40% saving) since FSSW requires no compressed air or water and no electrical transformation equipment [3, 4]. Nowadays, FSSW is widely used in automotive or aerospace industries.

The FSSW process consists of three main phases, typically, plunging phase, stirring phase and retracting phase [5]. In the plunging phase, the rotating tool penetrates in the weld spot until the shoulder reaches the desired depth in the surface of the upper sheet. In the stirring phase, the tool rotates in the workpiece without plunging. During the plunging and stirring phases, the frictional heat is generated. This heat softens both the upper and lower plates of the workpiece and causes the materials mix in the stirring phase. When the solid-state joint is produced, the process stops, and tool is retracted from the workpiece. The FSSW process parameters that affect the strength of the joints are reported as follows: the tool rotational speed, dwell time, plunge rate and plunge depth. Other parameters such as materials parameters (viz., alloy system, heat treatment…etc.), joint configurations and tool design play also an important role in determining the strength of the welded joints.

Optimization of FSSW parameters for similar metallic and non-metallic systems, using design of experiments approach, was reported by many workers [6, 9]. Using the optimization techniques allows the analysis of the experimental results and assists to better understand the effect of the FSSW process parameters on the mechanical and microstructural characteristics of the developed joints. In contrast, very few investigations about the optimization of FSSW similar Al alloys lap-joints were reports [10, 12]. While, according to our literature survey, no investigations were reported about the optimization of FSSW dissimilar Al alloys lap-joints.

The aim of the present investigation is to study the effect of FSSW process parameters, typically, the tool rotational speed, dwell time and plunging depth on the tensile-shear load of dissimilar AA1050-O/AA6061-T4 lap joints. It is required to determine the optimum range of the aforementioned FSSW parameters that maximize the tensile-shear load of these lap joints. Moreover, to estimate the contribution of individual FSSW parameters to the tensile-shear load of the weld joint. This was achieved using the analysis of variance (ANOVA) approach.

2. Experimental work

Sheets of the AA1050 and AA6061 wrought aluminum alloys were joined using FSSW. The chemical compositions of alloys are listed in Table 1. Large sheets with 2 mm thickness of the two alloys were cut into small pieces having dimensions of 100 mm length and 50 mm width. Before FSSW, the AA1050 and AA6061 sheets were heat treated to -O and -T4 conditions, respectively.

Table 1: Chemical composition the AA1050-O and AA6061-T4 aluminum alloys (wt.-%).

Alloy	Elements (wt. - %)							
	Si	Fe	Cu	Mn	Mg	Zn	Cr	Ti
AA1050-O	0.051	0.21	0.00942	0.00275	0.00432	0.0117	0.0001	0.00201
AA6061T4	0.552	0.0264	0.26	0.00434	1	0.00592	0.333	0.0245

The two sheets of AA1050-O/AA6061-T4 aluminum alloys are joined in a lap configuration as shown in Fig. 1. The AA6061-T4 and AA1050-O coupons were located at the

upper and lower positions of the joint, respectively. The FSSW was performed using a tool has a tapered pin profile and a concave shoulder as shown in Fig. 2. Table 2 lists the FSSW parameters used joining the AA1050-O/AA6061-T4 sheets.

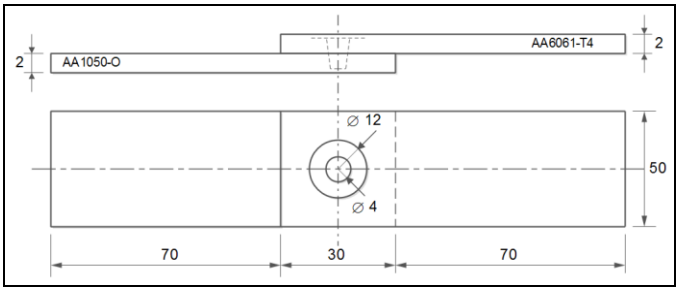

Fig 1: The AA1050-O/AA6061-T4 aluminum joints lap configuration (Dimensions in mm).

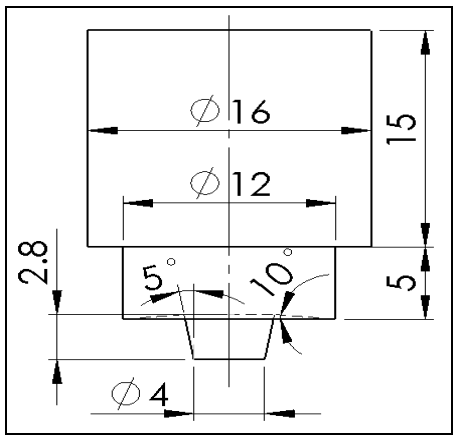

Fig 2: The FSSW tool (Dimensions in mm).

Table 2: The FSSW parameters and their levels.

Parameter	Level		
	Level 1 (min.)	Level 2 (avg.)	Level 3(max)
Rotational speed (rpm)	700	1120	1400
Dwell time (Sec.)	4	7	10
Plunging Depth (mm)	2.95	3.05	3.15

After FSSW, the welded joints were cut from cross-section from middle of welding spot for metallographic analysis. The samples were ground and polished using standard metallographic techniques. Microstructural examinations were conducted using optical microscopy. The macrostructural examinations were performed using image analyzing techniques. The macro- and micro-structural specimens were etched using Keller reagent. Tensile-shear tests were carried out using the specimens with the configuration shown in Fig. 1 using a universal testing machine at constant cross head of 1 mm/min. A minimum of three tests, from each FSSW condition, were carried out and the tensile-shear load was determined.

The full factorial design of experiments approach was adopted to design the FSSW experiments. The total number of FSSW conditions is $3^3 = 27$. The total runs for tensile shear test were 81 runs (27×3). The analysis of experimental results was carried out using the analysis of variance (ANOVA) statistical Approach. From results of ANOVA, the most and lowest significant FSSW parameters affecting the tensile strength of the welded joints can be determined. Moreover, the S/N (signal-to-noise) ratio was calculated using the average values by considering the quality characteristics the larger-the-better for the tensile-shear load of AA1050-O/AA6061-T4 welded joints.

Table 3: Fully factorial design of FSSW conditions.

Exp. No.	Rotational speed (RPM)	Dwell time (sec.)	Plunging Depth (mm)
1	710	4	2.95
2	710	4	3.05
3	710	4	3.15
4	710	7	2.95
5	710	7	3.05
6	710	7	3.15
7	710	10	2.95
8	710	10	3.05
9	710	10	3.15
10	1120	4	2.95
11	1120	4	3.05
12	1120	4	3.15
13	1120	7	2.95
14	1120	7	3.05
15	1120	7	3.15
16	1120	10	2.95
17	1120	10	3.05
18	1120	10	3.15
19	1400	4	2.95
20	1400	4	3.05
21	1400	4	3.15
22	1400	7	2.95
23	1400	7	3.05
24	1400	7	3.15
25	1400	10	2.95
26	1400	10	3.05
27	1400	10	3.15

3. Results and discussion

3.1 Weld structure characterization

Figure 3 shows photograph of typical AA1050-O/AA6061-T4 welded joint. The joint was welded using a rotational speed, dwell time and plunging depth of 1120 rpm, 7 sec. and 3.05 mm, respectively. Figure 4 shows micrographs of cross-sections of AA1050-O/AA6061-T4 welded lap joints produced using different FSSW conditions. The Al AA1050-O and AA6061-T4 polished surfaces have different gray levels due to different chemical compositions as shown in the Fig. 4. The AA6061-T4 upper Al sheet appears darker than the AA1050-O lower Al sheet. The AA6061-T4 upper and the AA1050-O lower sheets were compressed together during the plunging action of the pin resulting in a joint interface. This action also displaces a portion of the upper AA6061-T4 Al sheet decreasing its thickness. Moreover, the plunging of the concave shoulder extrudes a portion of the upper AA6061-T4 Al sheet, decreasing its thickness. The plunging action also bends the AA6061-T4 Al top sheet at the weld edge, creating a gap between the two Al sheets.

The stirred zone (SZ) is clearly seen in Fig. 4. In the SZ, the upper (AA6061-T4) and lower (AA1050-O) sheets are bonded

together. There is no clear interface between the heat affected zone (HAZ) and stir zone was observed from macrostructural examinations. The HAZ experienced a thermal cycle without any plastic deformation.

Fig 3: Photograph of a dissimilar AA1050-O/AA6061-T4 lap joint FSSW using 1120 rpm, 7 sec. and 3.05 mm.

(a)

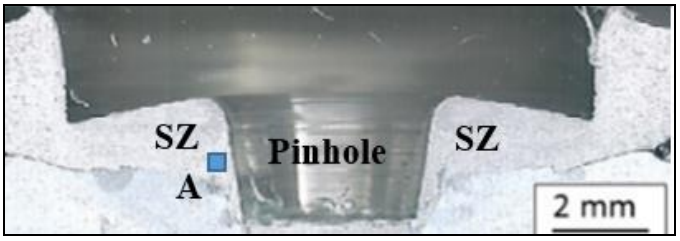

(b)

Fig 4: Macrographs of the cross-section of FSSW joints welded at (a) 1400 rpm, 4 sec. and 2.95 mm; and (b) 1400 rpm, 10 sec. and 3.15 mm.

3.2 Microstructural characterization

Figure 5 representative micrographs of the microstructure of SZs located at point A (see Fig. 4). The micrographs were taken from joints FSSW using constant tool rotational speed of 710 rpm and different dwell times and plunging depths. The SZs are characterized by very recrystallized grains structure of the primary α-Al grains. The variation of the average grain size at the SZs of with the plunging depth at different dwell times and tool rotational speeds is illustrated in Fig. 6. The results revealed that, at constant dwell time and plunging depth, increasing the tool rotational speed increases the average size of the α-Al grains at the SZs. For example, at constant dwell time and plunging depth of 7 sec. and 3.05 mm, respectively, increasing the tool rotational speed from 710 rpm to 1400 rpm increased the average grain size from 5 μm to 11 μm, respectively. It has been reported that at higher rotational speeds, a grain growth is taking place due to the rise in temperature generated in the stirred zone [11]. The effect of dwell time and plunging depth on the grain size at the SZs of AA1050-O/AA6061-T4 welded joints is not clear. Several investigations reported that the effect of FSSW process parameters on the microstructural and mechanical properties of Al joints is not yet fully understood since several contrary results regarding their effects were reported [1]. A minimum average grain size (≈ 4 μm) was observed for SZ of a joint welded using tool rotational speed, dwell time and plunging depth of 710 rpm, 4 sec. and 2.95 mm, respectively. While the maximum average grain size (≈ 13 μm) was observed for SZ of a joint welded using tool rotational speed, dwell time and plunging depth of 1400 rpm, 7 sec. and 3.15 mm, respectively.

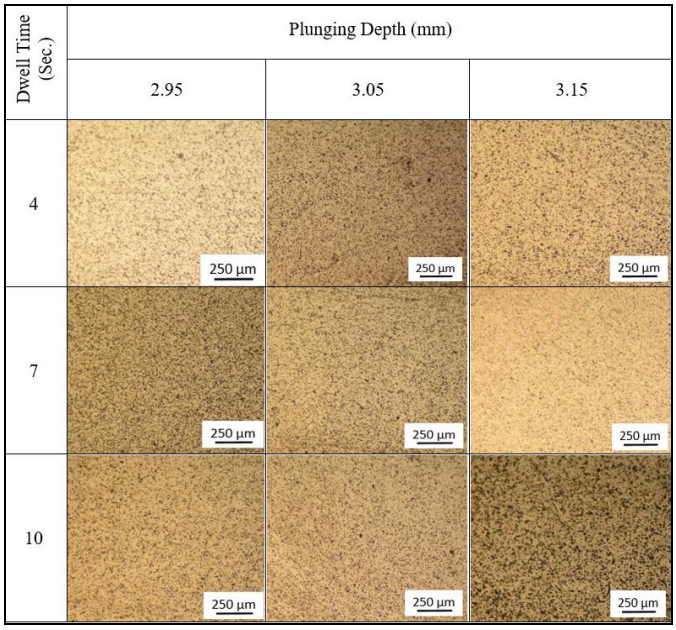

Fig 5: Micrographs of the microstructure of stirred zones from joints FSSW using constant tool rotational speed of 710 rpm and different dwell times and plunging depths.

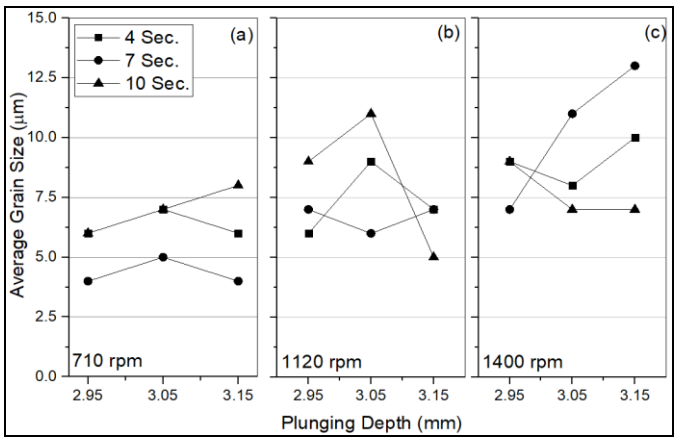

Fig 6: Variation of the average grains size of SZs of AA1050-O/AA6061-T4 lap joints with the plunging depth at different dwell times and tool rotational speeds. (a) 710 rpm, (b) 1120 rpm and (c) 1400 rpm.

3.3 Tensile-shear tests

Figure 7 shows the variation of the tensile-shear load of AA1050-O/AA6061-T4 lap joints with the plunging depth at different dwell times and tool rotational speeds. The results revealed that, at constant dwell time and plunging depth, increasing tool rotational speed reduces the tensile-shear load of the FSSW joints. This may be due to the grain growth that takes place due to the rise in temperature generated at higher

tool rotational speed. Again, there is no clear relationship between the FSSW process parameters such as the dwell time and plunging depth on the tensile-shear load of AA1050-O/AA6061-T4 lap joints.

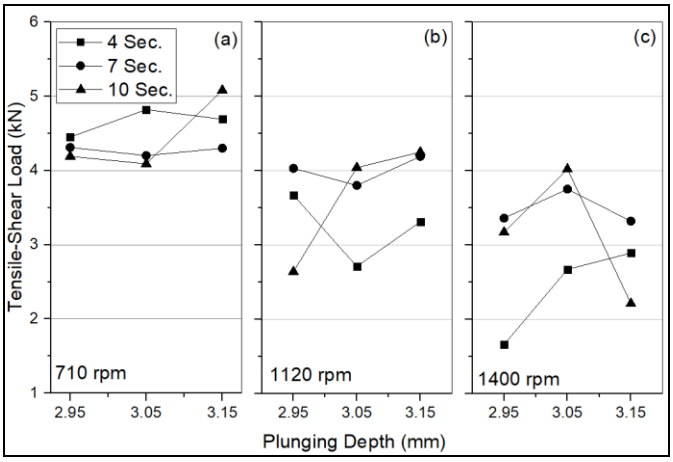

Fig 7: Variation of the tensile-shear load of AA1050-O/AA6061-T4 lap joints with the plunging depth at different dwell times and tool rotational speeds. (a) 710 rpm, (b) 1120 rpm and (c) 1400 rpm.

3.4 ANOVA results of tensile-shear load

The S/N ratios response table and response graph of the tensile-shear load for FSSW AA1050-O/AA6061-T4 lap joints resulted from ANOVA calculations are shown in Fig. 8 and Table 4, respectively. Based on the analysis of S/N ratios the optimum FSSW process parameter that maximize the tensile-shear load of FSSW AA1050-O/AA6061-T4 lap joints are obtained at tool rotational speed of 710 rpm (level 1), at dwell time of 7 sec. (level 2) and at plunging depth of 3.05 mm (level 2). This is can be concluded from Table 4, at which a greater S/N value corresponds to better tensile-shear load.

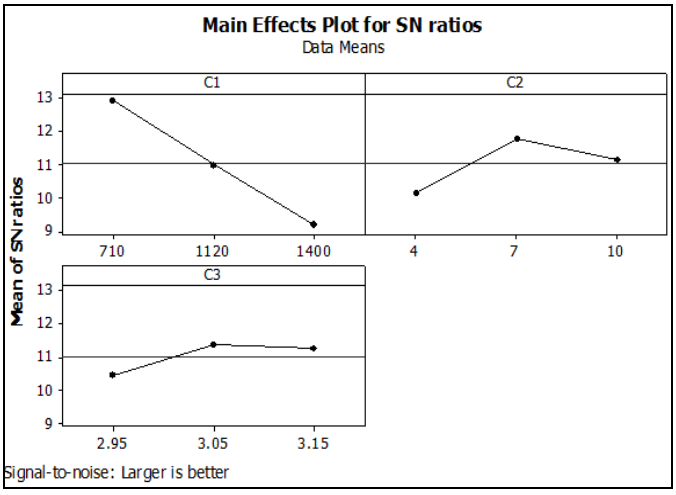

Fig 8: Main effects plot for S/N ratios for tensile-shear load.

Table 4: Response Table for Signal to Noise Ratios

Level	Rotational Speed	Dwell Time	Plunging Depth
1	12.907*	10.166	10.472
2	10.990	11.787*	11.358*
3	9.188	11.134	11.256
Delta	3.719	1.621	0.886
Rank	1	2	3

- Larger is better. * Optimum values.

Figure 9 shows the main effects plot for means for tensile-shear load of AA1050-O/AA6061-T4 lap joints. It it's clear that increasing the tool rotational speed from 710 rpm to 1400 rpm reduces the tensile shear load of the joints. While increasing the dwell time and/or the plunging depth to a certain level increase(s) the tensile-shear load. Further increase in dwell time and/or the plunging depth above this level tend(s) to reduce the tensile shear load. According to Fig. 9 these levels for the dwell time and the plunging depth are 7 sec. and 3.05 mm, respectively. Table 5 shows the results of the ANOVA for the tensile-shear load of AA1050-O/AA6061-T4 lap joints produced using FSSW. The analysis was carried out for a confidence limit of 95% (i.e. the level of significance is equal to 5%). From the analysis of Table 5, it can be concluded that the tool rotational speed has the most statistical and physical significance on the tensile-shear load of AA1050-O/AA6061-T4 lap joints, followed by the dwell time and then the plunging depth (see the Seq SS values in Table 5).

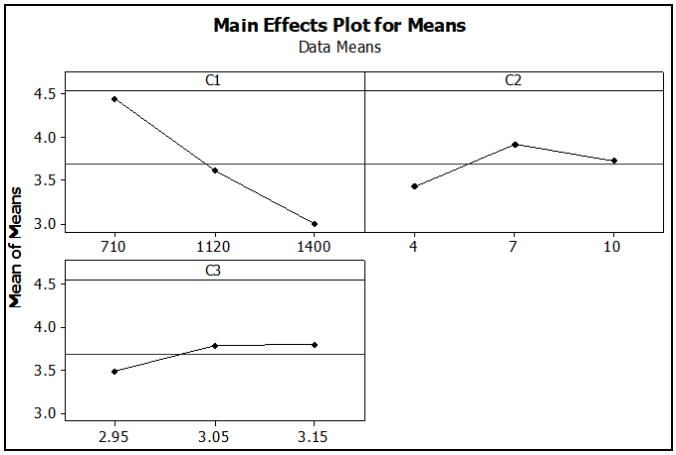

Fig 9: Main effects plot for means for tensile-shear load.

Table 5: ANOVA results for tensile-shear load.

Source	DF	Seq SS	Adj SS	Adj MS	F	P
Rotational speed	2	62.259	62.259	31.129	11.28	0.001
Dwell time	2	11.968	11.968	5.984	2.17	0.140
Plunging Depth	2	4.227	4.227	2.113	0.77	0.478
Residual Error	20	55.181	55.181	2.759		
Total	26	133.634				

4. Conclusions

Based on the results obtained from the present investigation, the following conclusions can be derived:

1. Increasing the tool rotational speed reduces the tensile-shear load of AA1050-O/AA6061-T4 lap joints produced using FSSW. No clear relationships between the dwell time and the plunging depth with the tensile-shear load were observed.
2. The tool rotational speed has the highest statistical and physical significance on the tensile-shear load of AA1050-O/AA6061-T4 lap joints produced using FSSW. The dwell time exhibited higher statistical and physical significance when compared with the plunging depth.
3. The optimum FSSW process parameter that maximize the tensile-shear load of FSSW AA1050-O/AA6061-T4 lap joints are obtained at tool rotational speed, dwell time and plunging depth of 710 rpm, 7 sec. and 3.05 mm, respectively.

5. Acknowledgments

The authors are thankful to the Benha University –Faculty of Engineering at Shoubra for providing the facilities and equipment used in the present investigation.

6. References

1. Mahmoud TS, Khalifa TA. Microstructural and Mechanical Characteristics of Aluminum Alloy AA5754 Friction Stir Spot Welds. Journal of Materials Engineering and Performance. 2014; 23(3):898-905.
2. Kulekc MK. Effects of Process Parameters on Tensile Shear Strength of Friction Stir Spot Welded Aluminium Alloy (En Aw 5005), Archives of Metallurgy and Materials. 2014; 59(1):221-224.
3. Sakano R, Murakami K, Yamashita K, Hyoe T, Fuzimoto M, Inuzuka M, *et al*. Development of spot FSW robot system for automotive body members, In: Proceedings of the 3rd international symposium of friction stir welding, Kobe, Japan, 2001.
4. Pierluigi Fanelli, Francesco Vivio, Vincenzo Vullo. Experimental and numerical characterization of Friction Stir Spot Welded joints, Engineering Fracture Mechanics. 2012; 81:17-25.
5. Afify RM, Mahmoud TS, Abd-Rabbo SM, Khalifa TA. On the microstructural and mechanical characteristics of friction stir spot welded AA1050-O aluminium alloys, MSAIJ. 2015; 13(7):226-236.
6. Mustafa Kemal Bilici. Application of Taguchi approach to optimize friction stir spot welding parameters of polypropylene, Technical Report, Materials and Design. 2012; 35:113-119.
7. Mustafa Kemal Bilici, Ahmet Irfan Yükler, Memduh Kurtulmus. The optimization of welding parameters for friction stir spot welding of high density polyethylene sheets, Materials and Design. 2011; 32:4074-4079.
8. Lakshminarayanan AK, Annamalai VE, Elangovan K. Identification of optimum friction stir spot welding process parameters controlling the properties of low carbon automotive steel joints, Journal of Materials Research and Technology. 2015; 4(3):262-272.
9. Kulekci MK, Esme U, Er O, Kazancoglu Y. Modeling and prediction of weld shear strength in friction stir spot welding using design of experiments and neural network Mat.-wiss. u. Wrest off tech. 2011; 42(11):990-995.
10. Merzoug M, Boulenouar A, Bouchouicha B, Serrier M, Mazari M. Effects of Welding Parameters on Fssw: Experimental and Numerical Study, Arch. Metall. Mater. 2018; 63(1):247-256.
11. Klobčar J, Tušek A, Skumavc A. Parametric study of friction stir spot welding of aluminium alloy 5754, Metalurgija. 2014; 53(1):21-24.
12. Merzoug M, Mazari M, Berrahal L, Imad A. Parametric studies of the process of friction spot stir welding of aluminium 6060-T5 alloys, Mater. 2010; 31(6):3023-3028.